ISJ 22: 91-106, 2025 ISSN 1824-307X

RESEARCH REPORT

Characterization of DDX21 gene and the association of its single nucleotide polymorphisms with susceptibility/resistance of *Magallana gigas* to *Halomonas sp. 7T*

Q Peng[1,2,3], T Liu[1,2,3], C Yang[1,2,3*], N Kong[1,2,3], B Wang[1,2,3], Y Wang[4], L Wang[1,2,3], L Song[1,2,3*]

[1]Liaoning Key Laboratory of Marine Animal Immunology & Disease Control, Dalian Ocean University, Dalian, 116023, China
[2]Liaoning Key Laboratory of Marine Animal Immunology, Dalian Ocean University, Dalian, 116023, China
[3]Dalian Key Laboratory of Aquatic Animal Disease Prevention and Control, Dalian Ocean University, Dalian, 116023, China
[4]School of Fisheries and Life Science, Dalian Ocean University, Dalian, 116023, China

This is an open access article published under the CC BY license *Accepted October 7, 2025*

Abstract

DEAD-box RNA helicase 21 (DDX21) is a widely expressed protein in cells, involved in almost all RNA-related cellular processes, and plays a significant role in disease prevention and defense within organisms. This study characterized a DDX21 in Pacific oyster *Magallana gigas* (*Mg*DDX21), and investigated its association of single nucleotide polymorphisms with susceptibility/resistance of oyster to *Halomonas sp. 7T*. *Mg*DDX21 contains three conserved domains (DEADc, HELICc, and GUCT), and shares highly conserved key functional sites with other organisms. High-temperature and Lipopolysaccharide (LPS) treatment both significantly upregulated the mRNA expression level of *Mg*DDX21 ($P < 0.05$). The promoter sequence of *Mg*DDX21 gene from the bacterial-resistant population and the common population was cloned, and the polymorphisms within this region were investigated by sequencing to analyze their association with bacterial resistance. A total of 25 single nucleotide polymorphism (SNP) sites were identified, and 21 SNPs and one haplotype TACACTAACT were significantly associated with the bacterial resistance trait of Pacific oyster, which could be used as potential markers for oyster selection breeding with higher bacterial resistance. These results lay the foundation for further investigation into the role of DDX21 in the response of Pacific oyster to bacterial resistance and provide candidate molecular markers for breeding new varieties of oysters with excellent disease resistance traits.

Key Words: *Magallana gigas;* DDX21; promoter; single nucleotide polymorphism; resistance to *Halomonas sp. 7T*

Introduction

RNA helicases are a family of proteins which utilize ATP to bind to or restructure RNA (Shih and Lee, 2014), and play important roles in various cellular processes, including transcription, ribosome assembly, mRNA translation, and the unwinding of double-stranded RNA (Valdez *et al*., 2002). They can be divided into five superfamilies (SF1-SF5) based on conserved protein sequences and domains. The SF2 superfamily subclass can be further divided into 10 families, among which the DExD/H helicase family contained several members, such as DEAD-box along with DEAH, DExH and DExD families (Cordin *et al*., 2006; Shih and Lee, 2014). DEAD-box helicases participate in the cell's defense against bacterial invasion by regulating various cellular processes, including DNA transcription, mRNA splicing, ribosome biogenesis, RNA transport, translation, degradation, cell cycle regulation, and miRNA biogenesis (Ma *et al.,* 2024).

DEAD-box RNA helicase 21 (DDX21) is a member of the DEAD-box helicase family (Flores-Rozas and Hurwitz, 1993; Calo *et al*., 2015; Zhou *et al*., 2024). Due to its significant roles in numerous cellular processes, there is growing interest in the relationship between DDX21 and biological immunity and disease resistance capabilities. The human DDX21 RNA helicase includes four conserved domains, DEADc, HELICc, GUCT_RHII, and the C-terminal FRGQR repeats (Flores-Rozas and Hurwitz, 1993). Moreover, there are 13 conserved motifs (Sarkar and Ghosh, 2016),

Corresponding authors:
Chuanyan Yang
Dalian Ocean University
52 heishijiao Street, Dalian 116023, China
E-mail: yangchuanyan@dlou.edu.cn
Linsheng Song
Dalian Ocean University
52 heishijiao Street, Dalian 116023, China
E-mail: lshsong@dlou.edu.cn

Table 1 Primers used in this study

Primer name	Sequence (5′-3′)	PCR objective
*Mg*DDX21-P1FO	5′-CCAATCCGAGACAGAAAGAAAATAG-3′	Promoter cloning
*Mg*DDX21-P1RO	5′-CAAGATTATCTGTTTTGAAACGCCC-3′	Promoter cloning
*Mg*DDX21-P1F	5′-GGAATCCACTCTCGTAACAAGC-3′	Promoter cloning
*Mg*DDX21-P1R	5′-ATGTCCCGAGTACTTCCGAATG-3′	Promoter cloning
*Mg*DDX21-P2FO	5′-TAACGCTGAGGGTAATAGAACGG-3′	Promoter cloning
*Mg*DDX21-P2RO	5′-ATGGCTTACCTGAACGCTGACC-3′	Promoter cloning
*Mg*DDX21-P2F	5′-TCTGTCTCAAGTTATTGCTTCCATC-3′	Promoter cloning
*Mg*DDX21-P2F	5′-CATATCCCTATCGTTATTCTTTTGC-3′	Promoter cloning
*Mg*DDX21-RT-F	5′-CCCTCGGTGATTGGTGATGTGCT-3′	qRT-PCR
*Mg*DDX21-RT-R	5'-CGTGTAATACTTGAGCGTCCTGC-3'	qRT-PCR
Mg-EF-RT-F	5'-AGTCAccAAGGCTGCACAGAAAG-3’	qRT-PCR
Mg-EF-RT-R	5'-TCATATTTCTTTGATGT-3’	qRT-PCR

among which, motifs I and II are core motifs, and the conserved sequence (D-E-A-D, Asp-Glu-Ala-Asp) is located within motif II (Fairman-Williams *et al*., 2010). DDX21 is a nucleolar protein that binds and promotes the transcription, processing, and modification of RNA (Flores-Rozas and Hurwitz, 1993; Calo *et al*., 2015). Recently, several studies have shown its involvement in regulating antiviral immune response, the development of cancer, and innate immunity of cells. DDX21 could inhibit viral genome replication and suppress the assembly and release of viral particles through multiple mechanisms (Abdullah *et al*., 2021), and its high expression in most cancers was positively correlated with cell proliferation and migration ability (Hu *et al*., 2022). Furthermore, DDX21 can maintain innate immune homeostasis by negatively regulating the production of IFN-b (Li *et al*., 2022). In recent years, a significant number of studies have indicated that polymorphisms in the gene sequences of some DEAD-box family members are associated with disease occurrence, providing clues for understanding biological diseases and prevention mechanisms. For instance, SNPs in DEAD box polypeptide 5 (DDX5) was found to increase the risk of advanced fibrosis and bloom syndrome (Bamezai, 1996; Guo *et al*., 2010). However, there is less research on the relationship with genetic sequence polymorphisms of DDX21 gene and disease.

So far, research on the function of DDX21 has been primarily focused on mammals, and there are no relevant studies reported in the field of aquatic animals. Nevertheless, numerous reports indicated that other members of the DEAD box family are pivotal in life processes such as cell division, antiviral immune defense, and individual development in aquatic animals (Yajima and Wessel, 2011; Gan *et al*., 2020; Tseng *et al*., 2021). For instance, Vasa, one member of the DEAD-box RNA helicase family, disrupts chromosome segregation, resulting in cells arresting at the M phase and thereby impeding the progression of the entire cell cycle (Yajima and Wessel, 2011). Additionally, overexpression of DDX41 in *Nile tilapia* can lead to strong activation of the promoters of type I interferons, thereby triggering the cell's antiviral immune response (Gan *et al*., 2020). Interestingly, disrupting the RNA helicase DDX52 expression could lead to a transient pause in the development of zebrafish larvae, and this developmental arrest is largely reversible (Tseng *et al*., 2021). These studies suggest that DDX21, as a member of the DEAD-box RNA helicase family, may also play a significant role in immune processes.

The Pacific oyster *Magallana gigas* (previously known as *Crassostrea gigas*), a marine aquaculture bivalve highly favored for its ecological and economic benefits, is a significant species in northern China's aquaculture industry. However, in recent years, large-scale mortality events caused by combined action of microbial pathogens and the environment frequently occurred in *M. gigas* farms. In the spring of 2020, a local oyster farm in Zhuanghe, Liaoning Province, experienced an outbreak of 'Red Shell Disease' among its larvae, resulting in substantial losses for the oyster industry. The causative pathogen was subsequently identified as *Halomonas* sp. *7T* (Li, 2022). Considering that RNA helicase DDX21 likely participates in immune response and regulation processes, we investigated

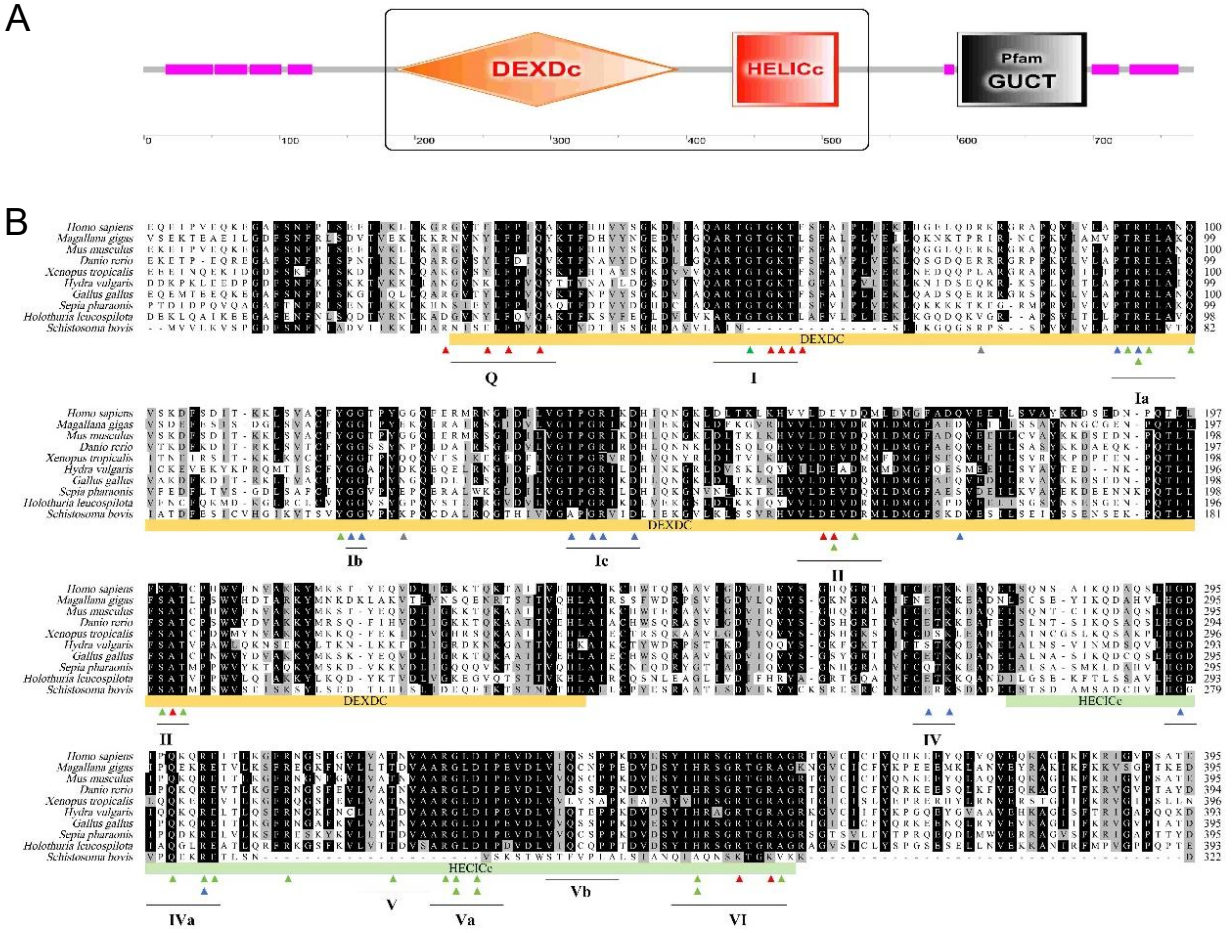

Fig. 1 Domain composition (A) and multiple sequence alignment (B) of the *Mg*DDX21 protein sequence with the DDX21 sequences from other species. The black boxes and the areas enclosed by them correspond to the sequence positions compared in B, where red, blue, and green triangles represent residues involved in ATP binding, RNA binding, and domain-domain interactions, respectively

the sequence structure, expression and genetic polymorphism characteristics of oyster *Mg*DDX21, aimed to (1) clarify its structural characteristics, (2) explore its expression profile after high-temperature and lipopolysaccharide (LPS) stimulation, and (3) find a correlation between the population-specific molecular characteristics of the *Mg*DDX21 gene promoter and the different susceptibility/resistance of *M. gigas* to *Halomonas* sp. *7T*.

Materials and methods

Animals, treatment, and sample collection

In this study, the Pacific oysters *M. gigas* (about 10.0 cm in shell length) were collected from a local farm in Zhuanghe, Liaoning Province, China. The oysters were acclimated using the same method as previously employed in the laboratory (Wu *et al*., 2023). Haemocytes and tissues including gill, gonad, hepatopancreas, adductor muscle and mantle were collected from six oysters as parallel samples. After the addition of 1 mL Trizol reagent (Invitrogen), all the samples were stored at -80 °C for RNA extraction.

In the high-temperature treatment experiment, 63 oysters were randomly selected and treated in high-temperature seawater at 28 °C. Nine oysters were randomly selected at 0, 3, 6, 12, 24, 48, and 72 h, respectively, and haemolymph was collected for RNA extraction.

In the LPS stimulation experiment, 108 oysters were randomly divided into two groups. After injections with sterile seawater (SW) and LPS, nine oysters were randomly sampled from each group at 0, 3, 6, 12, 24, and 48 h. Haemolymph was collected for RNA extraction. The injections with SW and LPS, as well as the extraction of RNA from haemocytes, were carried out according to previous laboratory protocols (Wu *et al*., 2023).

Total RNA isolation, cDNA synthesis and gene cloning were performed according to previous reports (Wang *et al*., 2016). The genomic DNA for SNP detection was extracted from the adductor muscles using a TIANamp Marine Animals DNA kit (Tiangen Biotech, Beijing, China). The integrity of the extracted DNA was evaluated by agarose gel electrophoresis.

Two populations, the *Halomonas sp. 7T*-resistant

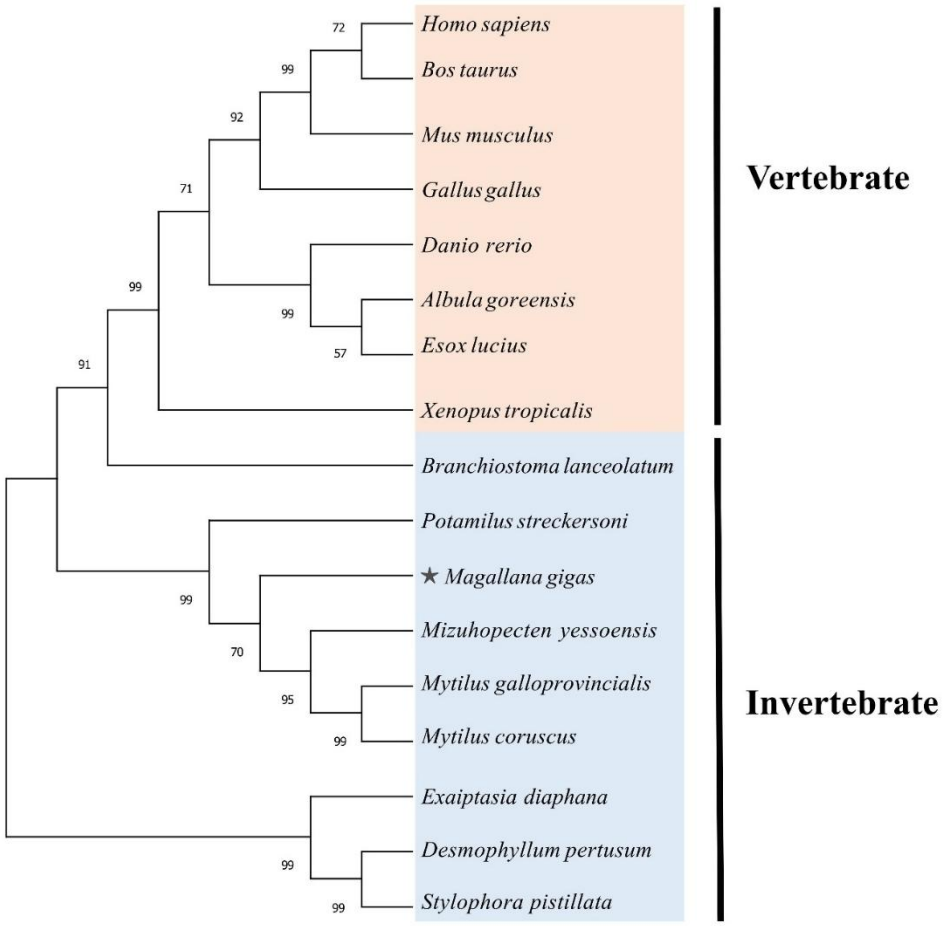

Fig. 2 Phylogenetic tree based on alignment of the *Mg*DDX21 protein sequence and the DDX21 sequences from other species. The numbers at the nodes indicate the bootstrap values

population (bacterial resistant population) and the common population, were used for screening SNP in the promoter of *Mg*DDX21. The resistance population refers to the F2 generation oysters obtained after challenging F1 and F2 juvenile oysters with *Halomonas* sp *7T* (duration: 72 h; concentration: 10^7 cells/mL) during family establishment (unpublished data). Wild populations that have not undergone artificial breeding were used as the common population. An additional *Halomonas sp. 7T* challenge test was carried out on the resistant population and the common population, and the results showed that the resistant population exhibited a significantly higher survival rate and reached a stable state earlier than the common population, indicating superior tolerance to this bacterial strain. The adductor muscle of each oyster from two populations was removed and kept at -80 °C until DNA isolation.

Sequence analysis of Mg*DDX21*

The conserved domains of *Mg*DDX21 were predicted using the simple modular architecture research tool (SMART) (http://smart.embl-heidelberg.de/). The amino acid sequence analyses were carried out using the BLAST algorithm (http://www.ncbi.nlm.nib.gov/BLAST). The neighbor-joining (NJ) phylogenetic tree of *Mg*DDX21 was constructed using MEGA version X software. Bootstrap trials were replicated 1000 times to derive the confidence value for phylogeny analysis. According to relevant reports (Chen *et al*., 2020), through multiple sequence alignments of *Mg*DDX21 with other species using the MEGA software, key functional sites were identified.

Quantitative Real-time PCR analysis of Mg*DDX21 mRNA expression*

The SYBR Green qRT-PCR was carried out on an ABI 7500 Real-time Thermal Cycler platform according to the manufacturer's protocol (TaKaRa). All primers used in this assay were listed in Table 1. The *Mg*EF-α gene (GenBank accession No. NW_018406511.1) was employed as internal control, and the relative expression levels of *Mg*DDX21 were analyzed using the comparative Ct method ($2^{-\Delta\Delta Ct}$ method). Data were statistically analyzed through one-way ANOVA followed by multiple comparisons. Significant differences were accepted at $P < 0.05$.

Cloning and sequence analysis of Mg*DDX21 promoter*

The primers for *Mg*DDX21 (Table 1) were designed according to the sequence information of *Mg*DDX21 (GenBank accession LOC105343804) for cloning promoter sequence, and the promoter region sequence of *Mg*DDX21 was cloned using nested PCR. The PCR product was gel-purified, cloned into pMD19-T simple vector (Takara), and confirmed by DNA sequencing.

The promoter sequence of *Mg*DDX21 was analyzed using the Transcription Element Search System (TESS) (http://www.cbil.upenn.edu/tess/) and the Patch System (http://www.generegulation.com/cgibin/pub/programs/patch/bin/patch.cgi?). The possible transcription start site was predicted using the Neural Network Promoter Prediction (NNPP) (http://www.fruitfly.org/seq_tools/promoter.html).

Identification of SNPs in the promoter region of Mg*DDX21*

According to the promoter sequence of *Mg*DDX21, two sets of gene-specific primers (Table 1) were designed to amplify a 2272 bp fragment through nested PCR. The PCR products were excised, purified, cloned into pMD19-T vector (TaKaRa) and sequenced as previously reported (Yang *et al*., 2014). The alignments of nucleotide sequence of the *Mg*DDX21 promoter region were performed using DNAMAN version 6, and the polymorphisms in promoter region were identified from the sequence alignments of different individuals.

Association analysis of SNPs with resistance of oyster to Halomonas *sp. 7T*

The genomic DNA (100 ng μL^{-1}) of 30 individuals from each population was used as template to amplify the promoter region. The PCR products were subsequently sent to a biotechnology company for sequencing. SNPs identified in the promoter region were screened by sequencing to examine their association with susceptibility/resistance of oysters to *Halomonas* sp *7T*.

The genotype data was analyzed to test Hardy-Weinberg equilibrium (HWE). Moreover, linkage disequilibrium (LD) test and haplotype analysis were also conducted according to the genotyping results. All the data were analyzed by using SHEsis software (http://analysis.bio-x.cn). Significant differences were accepted at $P < 0.05$.

Statistical analysis

All statistical analyses were performed using IBM SPSS Statistics version 25. Differences among groups were evaluated by one-way ANOVA, followed by multiple comparisons with the LSD (least significant difference) test. Differences were considered significant at $P < 0.05$.

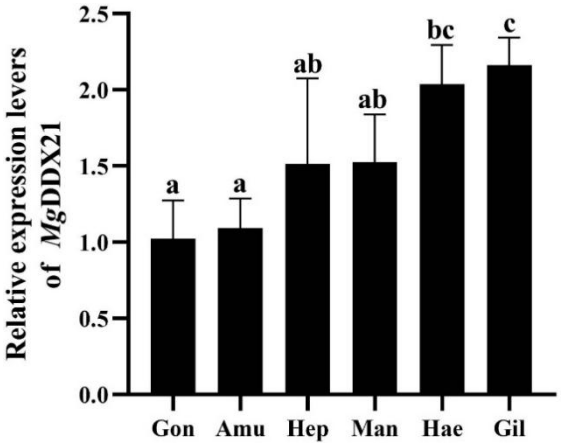

Fig. 3 The relative *Mg*DDX21 mRNA expression in different tissues. Vertical bars represent the mean ± S.E. (N ≥ 4). Differences labeled with different letters were statistically significant

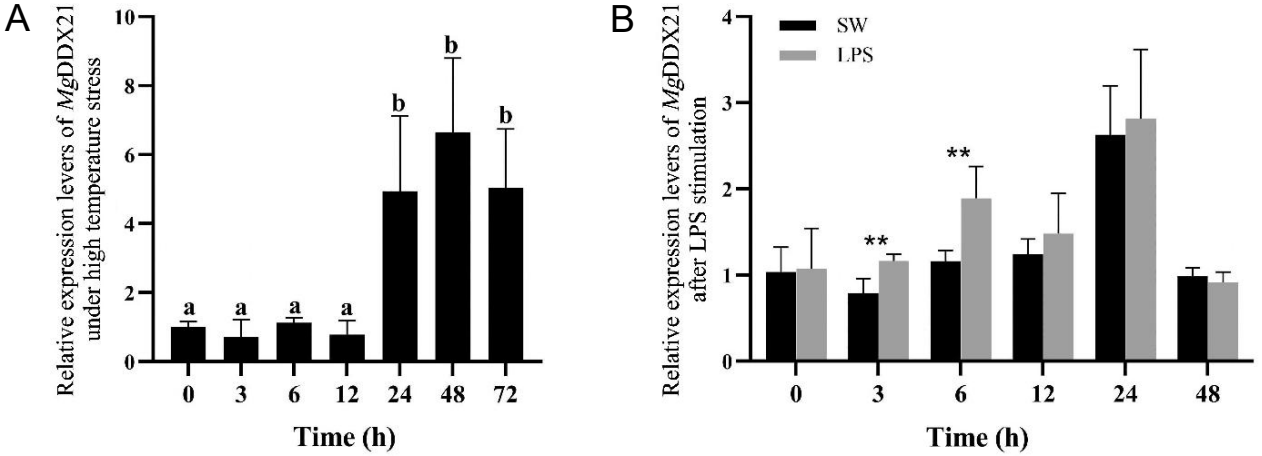

Fig. 4 The relative expression of *Mg*DDX21 mRNA in haemocytes after stimulation with high temperature and LPS for different durations. Vertical bars represent the mean ± S.E. (N ≥ 4). Differences labeled with different letters (A) or * (B) were statistically significant

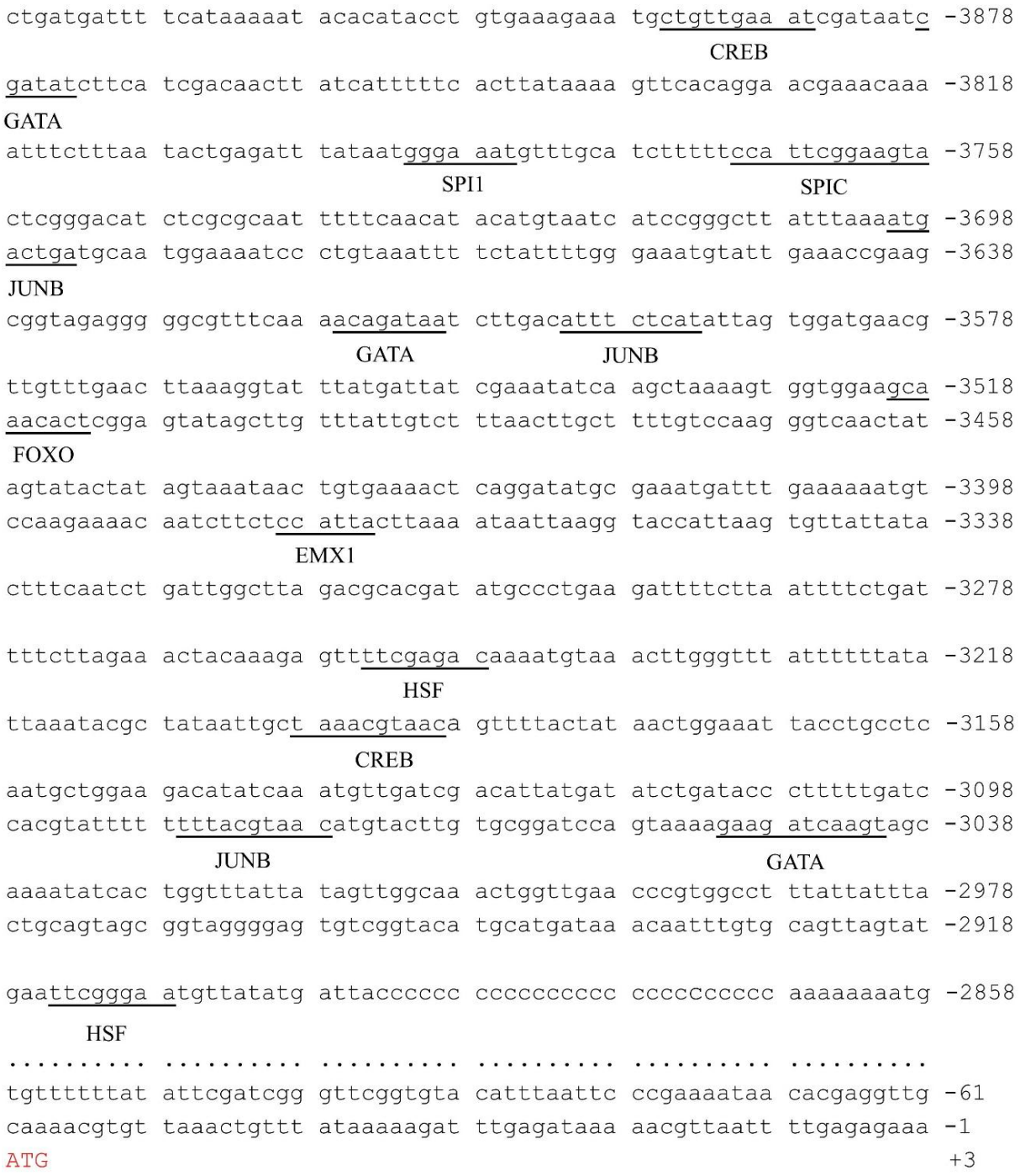

Fig. 5 Sequence analysis of *Mg*DDX21 promoter. The negative numbers on the right indicate upstream sequence relative to the translation start codon, and the putative transcription factor binding sites ware underlined

Result

Sequence characteristics and phylogenetic evolution of Mg*DDX21*

The open reading frame (ORF) of *Mg*DDX21 was of 2325 bp, encoding a polypeptide of 774 amino acid residues with an isoelectric point of 9.12 and a molecular weight of 86.1 kDa. Using the SMART website for domain prediction, it was found that *Mg*DDX21 contains three conserved domains: DEADc, HELICc, and GUCT (Fig. 1A).

The protein sequence of *Mg*DDX21 was aligned with DDX21 protein sequences obtained from other species in the NCBI database. The results indicate that *Mg*DDX21 shows relatively low similarity (20.75%-39.62%) to DDX21 proteins from various species. By conducting multiple sequence alignments, it has been noted that motifs characteristic of higher

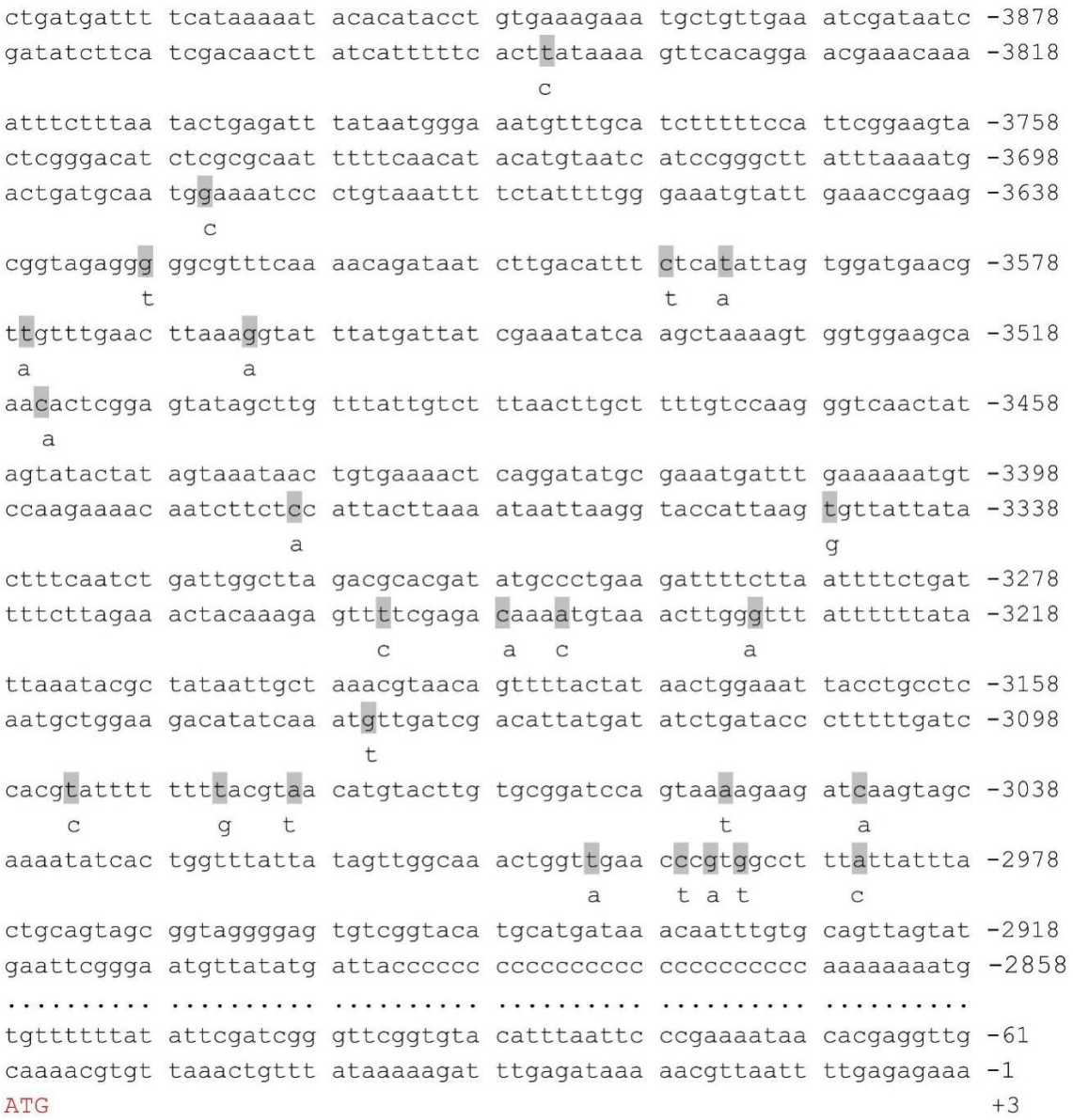

Fig. 6 The SNPs in the promoter region of *Mg*DDX21. The negative numbers indicate upstream sequence relative to the translation start codon and are numbered on the right. The polymorphic sites are underlined, and the variants are described below

animals (Q, I, Ia, Ib, Ic, II, IV, IVa, V, Va, Vb and VI) are also significantly present in *Mg*DDX21 (Fig. 1B).

The phylogenetic trees were constructed to analyze the phylogenetic evolution of DDX21s. *Mg*DDX21 gathered with the DDX21s from the other molluscs (*Mizuhopecten yessoensis*, *Mytilus galloprovincialis*, *Mytilus coruscus*, and *Potamilus streckersoni*). *Mg*DDX21 shared relatively far evolutionary relationships with DDX21s from Cnidarias (*Desmophyllum pertusum* and *Stylophora pistillata*) (Fig. 2).

The distribution of Mg*DDX21 mRNA in different tissues and haemocytes*

*Mg*DDX21 was expressed in haemocytes and all tested tissues including gills, mantle, adductor muscle, hepatopancreas, and gonad (Fig. 3). The highest expression was observed in gills, which was 2.11-fold of that in the gonads ($P < 0.05$). Furthermore, the expression levels in haemocytes were notably higher than that in gonad (1.99-fold, $P < 0.05$).

Mg*DDX21 expression in response to high-temperature and LPS*

The expression of *Mg*DDX21 mRNA was assessed to evaluate its activation under high temperature stress (28°C) and after LPS stimulation. After high temperature treatment, the *Mg*DDX21 mRNA expression in haemocytes significantly increased at 24 h (4.90-fold of that at 0 h, $P < 0.05$), peaking at 48 h (6.60-fold of that at 0 h, $P < 0.05$),

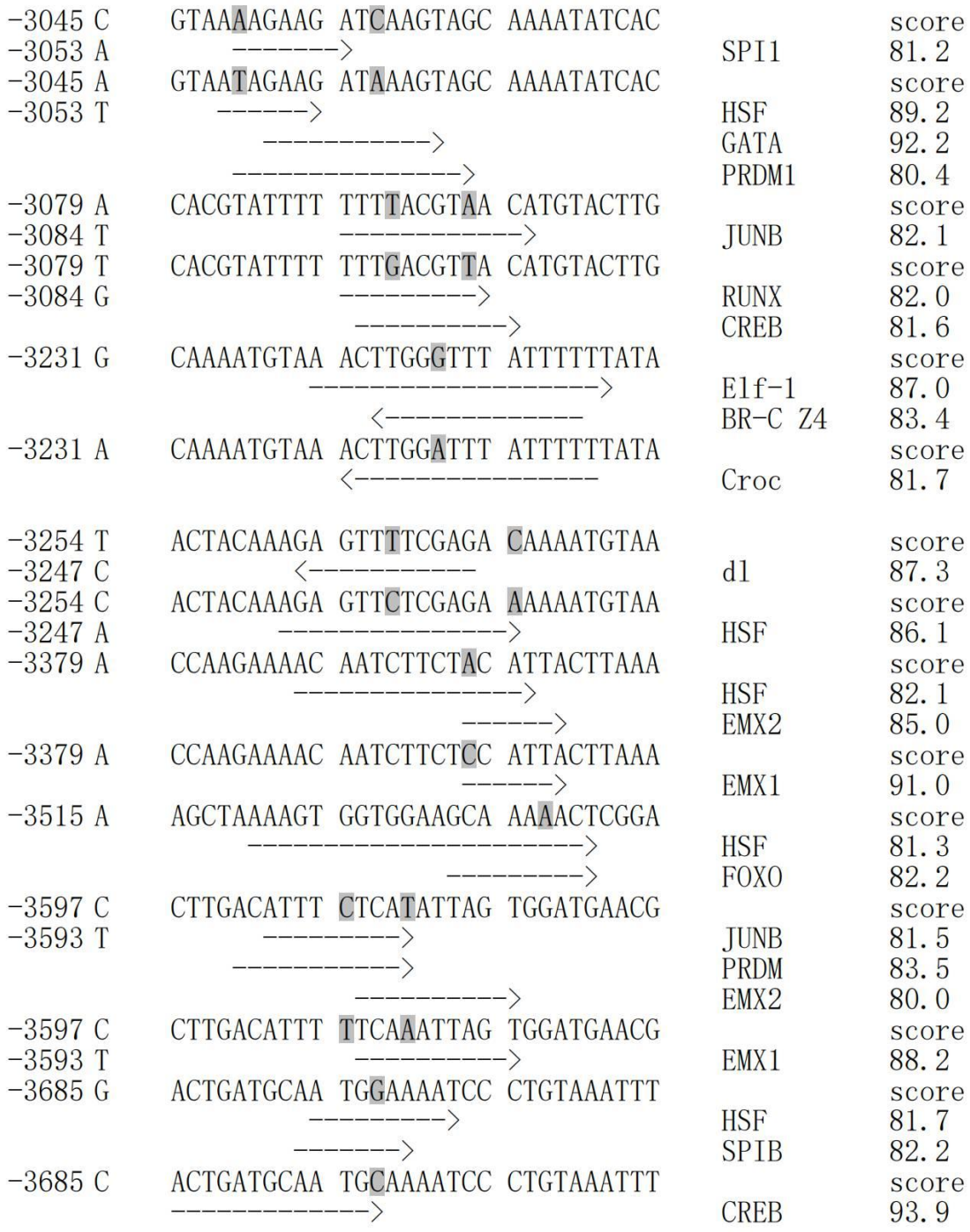

Fig. 7 Difference of putative binding sites for transcription factors between different alleles. Polymorphic loci are shadowed in gray, and the first polymorphic locus of each line is numbered on the left. The positions and directions of putative binding sites for transcription factors are labeled by the arrowhead. The TFSEARCH scores are shown on the right

and remained significantly upregulated at 72 h (5.00-fold of that at 0 h, $P < 0.05$) (Fig. 4A).

Comparatively, the *Mg*DDX21 mRNA expression was relatively flat after LPS stimulation, which was significantly up-regulated at 3 h and 6 h after stimulation (1.47-fold and 1.63-fold of that in the control group, respectively, $P < 0.05$) (Fig. 4B).

The sequence features of Mg*DDX21 promoter*

A remote promoter region sequence of 2272 bp was successfully cloned using PCR technology. The A, T, G, and C base content of *Mg*DDX21 promoter region was 32.6%, 33.0%, 17.0% and 17.4%, respectively, indicating that the cloned promoter region was an AT rich region (65.6%) (Fig. 5).

Table 2 Hardy-Weinberg equilibrium analyses (HWE) of twenty-five SNPs in *Mg*DDX21 detected in the two populations

Name	df	Bacterial-resistant population		Common population	
		Chi-squared	*P*-value	Chi-squared	*P*-value
-3844 C/T	1	19.49	$P < 0.05$	22.14	$P < 0.05$
-3685 C/G	1	38.00	$P < 0.05$	27.02	$P < 0.05$
-3628 T/G	1	37.00	$P < 0.05$	0	$P > 0.05$
-3597 T/C	1	28.93	$P < 0.05$	33.00	$P < 0.05$
-3593 A/T	1	30.24	$P < 0.05$	12.56	$P < 0.05$
-3576 A/T	1	38.00	$P < 0.05$	13.22	$P < 0.05$
-3562 A/G	1	30.35	$P < 0.05$	0	$P > 0.05$
-3515 A/C	1	33.00	$P < 0.05$	26.38	$P < 0.05$
-3379 A/C	1	46.07	$P < 0.05$	43.00	$P < 0.05$
-3347 G/T	1	14.53	$P < 0.05$	10.68	$P < 0.05$
-3254 C/T	1	10.94	$P < 0.05$	43.00	$P < 0.05$
-3247 A/C	1	34.26	$P < 0.05$	42.00	$P < 0.05$
-3243 C/A	1	30.02	$P < 0.05$	42.00	$P < 0.05$
-3231 A/G	1	23.65	$P < 0.05$	46.00	$P < 0.05$
-3135 T/G	1	42.00	$P < 0.05$	0.02	$P > 0.05$
-3093 C/T	1	23.40	$P < 0.05$	0	$P > 0.05$
-3084 G/T	1	16.41	$P < 0.05$	33.00	$P < 0.05$
-3079 T/A	1	28.00	$P < 0.05$	0	$P > 0.05$
-3053 T/A	1	28.00	$P < 0.05$	0	$P > 0.05$
-3045 A/C	1	12.78	$P < 0.05$	0	$P > 0.05$
-3001 A/T	1	28.00	$P < 0.05$	0	$P > 0.05$
-2996 T/C	1	28.00	$P < 0.05$	0	$P > 0.05$
-2994 A/G	1	35.81	$P < 0.05$	32.48	$P < 0.05$
-2992 T/G	1	27.00	$P < 0.05$	0	$P > 0.05$
-2985 G/A	1	26.00	$P < 0.05$	0.01	$P > 0.05$

Several putative cis-regulatory elements were identified in DDX21, including JUNB (3), GATA (3), HSF (2), CREB (2), and one each of SPI1 (1), FOXO (1), SPIC (1), and EMX1 (1) elements (Fig. 5).

The polymorphisms in the promoter region of Mg*DDX21*

A total of 25 SNP loci were identified within the amplified promoter region of *Mg*DDX21 (2272 bp), including -3844 C/T, -3685 C/G, -3628 G/T, -3597 C/T, -3593 T/A, -3576 T/A, -3562 A/G, -3515 C/A, -3379 A/C, -3347 G/T, -3254 T/C, -3247 A/C, -3243 A/C, -3231 G/A, -3135 G/T, -3093 T/C, -3084 T/G, -3079 A/T, -3053 A/T, -3045 A/C, -3001 T/A, -2996 C/T, -2994 A/G, -2992 G/T, -2985 A/C (Fig. 6).

The potential transcription factor binding sites at these 25 loci was analyzed using the JASPAR website, and the identical parts were excluded. A total of 12 sites were found to have differences (Fig. 7). At four loci (-3045, -3247, -3515 and -3597), there were some more putative transcription factor binding sites in one allele than their corresponding allele. For example, there were two more putative binding site for GATA and PRDM1 in A allele than C allele at locus -3045, and there was one more putative binding site for HSF in A allele than C allele at locus -3247. At the other eight loci (-3053, -3084, -3079, -3231, -3254, -3379, -3593, and -3685), the polymorphisms changed the respective transcription factor binding sites in each allele. For example, at the -3053 locus, the A allele has an additional SPI1 binding site compared to the T allele, while the T allele has an additional SPI1 binding site compared to the A allele. At the -3084 loci, the T allele have more JUNB transcription binding sites than the G allele, while the G allele have more RUNX and CREB

Table 3 Distribution of different genotypes at twenty-five SN*P* sites of *Mg*DDX21 in the common and bacterial-resistant populations

Name	Genotype	No. (%)		$\chi^2(P)$	Allele	No. (%)		$\chi^2(P)$
		Common population	Bacterial-resistant Population			Common population	Bacterial-resistant Population	
-3844 C/T	CC	19(0.39)	2(0.04)	24.12($P < 0.05$)	C	46(0.47)	6(0.06)	37.93($P < 0.05$)
	CT	8(0.16)	2(0.04)					
	TT	22(0.45)	43(0.92)		T	52(0.53)	88(0.94)	
-3685 G/C	GG	39(0.90)	22(0.58)	11.67($P < 0.05$)	G	78(0.91)	44(0.58)	23.35($P < 0.05$)
	GC	0(0)	0(0)					
	CC	4(0.10)	16(0.42)		C	8(0.09)	32(0.42)	
-3628 G/T	GG	44(1)	32(0.86)	4.22($P < 0.05$)	G	88(1)	64(0.86)	10.45($P < 0.05$)
	TT	0(0)	5(0.14)		T	0(0)	10(0.14)	
-3597 C/T	CC	38(0.90)	22(0.58)	11.29($P < 0.05$)	C	76(0.90)	44(0.58)	6.91（$P>0.05$）
	TT	4(0.10)	16(0.42)		T	8(0.01)	32(0.42)	
-3593 T/A	TT	44(0.96)	33(0.87)	1.12($P>0.05$)	T	88(0.96)	66(0.87)	3.15($P>0.05$)
	AA	2(0.04)	5(0.13)		A	4(0.04)	10(0.13)	
-3576 T/A	TT	41(0.89)	22(0.58)	19.03($P < 0.05$)	T	85(0.92)	44(0.58)	25.88($P < 0.05$)
	TA	3(0.07)	0(0)					
	AA	2(0.04)	16(0.42)		A	7(0.08)	32(0.42)	
-3562 A/G	AA	0(0)	5(0.14)	6.61($P < 0.05$)	A	0(0)	10(0.13)	13.23($P < 0.05$)
	GG	46(1)	32(0.86)		G	92(1)	64(0.87)	
-3515 C/A	CC	38(0.90)	22(0.67)	6.55($P < 0.05$)	C	76(0.90)	44(0.67)	13.10($P < 0.05$)
	AA	4(0.10)	11(0.33)		A	8(0.10)	22(0.33)	
-3379 A/C	AA	3(0.07)	23(0.46)	15.60($P < 0.05$)	A	6(0.07)	46(0.46)	33.05($P < 0.05$)
	CC	40(0.93)	27(0.54)		C	80(0.93)	54(0.54)	
-3347 G/T	GG	19(0.43)	2(0.04)	36.58($P < 0.05$)	G	50(0.57)	7(0.07)	52.66($P < 0.05$)
	GT	12(0.27)	3(0.06)					
	TT	13(0.3)	45(0.9)		T	7(0.07)	93(0.93)	
-3254 T/C	TT	39(0.91)	23(0.48)	20.68($P < 0.05$)	T	78(0.91)	58(0.6)	20.45($P < 0.05$)
	TC	0(0)	12(0.25)					
	CC	4(0.09)	13(0.27)		C	8(0.09)	38(0.4)	
-3247 A/C	AA	1(0.02)	21(0.43)	23.02($P < 0.05$)	A	3(0.04)	46(0.47)	40.06($P < 0.05$)
	AC	1(0.02)	4(0.08)					
	CC	39(0.96)	24(0.49)		C	79(0.96)	52(0.53)	

Name	Genotype	No. (%)		$\chi2(P)$	Allele	No. (%)		$\chi2(P)$
		Common population	Bacterial-resistant Population			Common population	Bacterial-resistant Population	
-3243 A/C	AA	40(0.95)	23(0.48)	24.02($P < 0.05$)	A	80(0.95)	51(0.53)	38.01($P < 0.05$)
	AC	0(0)	5(0.1)					
	CC	2(0.05)	20(0.42)		C	4(0.05)	45(0.47)	
-3231 G/A	GG	45(0.94)	24(0.5)	23.19($P< 0.05$)	G	90(0.94)	55(0.57)	32.57($P< 0.05$)
	GA	0(0)	7(0.15)					
	AA	3(0.06)	17(0.35)		A	6(0.06)	41(0.43)	
-3135 G/T	GG	43(0.96)	37(0.88)	7.36($P< 0.05$)	G	88(0.98)	74(0.88)	4.93($P< 0.05$)
	GT	2(0.04)	0(0)					
	TT	0(0)	5(0.12)		T	2(0.02)	10(0.12)	
-3093 T/C	TT	42(1)	36(0.82)	8.42($P< 0.05$)	T	84(1)	75(0.85)	11.39($P< 0.05$)
	TC	0(0)	3(0.07)					
	CC	0(0)	5(0.11)		C	0(0)	13(0.15)	
-3084 T/G	TT	16(0.48)	24(0.82)	12.79($P< 0.05$)	T	32(0.48)	48(0.92)	25.58($P< 0.05$)
	TG	0(0)	0(0)					
	GG	17(0.52)	2(0.08)		G	34(0.52)	4(0.08)	
-3079 A/T	AA	34(1)	23(0.82)	4.42($P< 0.05$)	A	68(1)	46(0.82)	10.91($P< 0.05$)
	TT	0(0)	5(0.18)		T	0(0)	10(0.18)	
-3053 A/T	AA	34(1)	23(0.82)	4.42($P< 0.05$)	A	68(1)	46(0.82)	10.91($P< 0.05$)
	TT	0(0)	5(0.18)		T	0(0)	10(0.18)	
-3045 A/C	AA	0(0)	5(0.19)	5.90($P< 0.05$)	A	0(0)	10(0.19)	11.79($P< 0.05$)
	AC	0(0)	0(0)					
	CC	29(1)	22(0.81)		C	58(1)	44(0.81)	
-3001 T/A	TT	26(1)	23(0.79)	4.10($P< 0.05$)	T	52(1)	46(0.79)	10.04($P< 0.05$)
	AA	0(0)	6(0.21)		A	0(0)	12(0.21)	
-2996 C/T	CC	27(1)	22(0.81)	3.53($P>0.05$)	C	54(1)	44(0.81)	8.93($P< 0.05$)
	TT	0(0)	5(0.19)		T	0(0)	10(0.19)	
-2994 A/G	AA	5(0.13)	5(0.19)	1.05($P>0.05$)	A	10(0.13)	10(0.19)	0.194(P>0.05)
	GG	33(0.87)	22(0.81)		G	66(0.87)	44(0.81)	
-2992 G/T	GG	27(1)	15(0.56)	12.96($P< 0.05$)	G	54(1)	30(0.56)	28.34($P< 0.05$)
	TT	0(0)	12(0.44)		T	0(0)	24(0.44)	
-2985 A/C	AA	28(1)	21(0.81)	5.93($P< 0.05$)	A	56(1)	42(0.81)	11.97($P< 0.05$)
	GG	0(0)	5(0.19)		G	0(0)	10(0.19)	

potential binding sites compared to the T allele. The nucleotides are numbered on the left. The polymorphism sites are underlined, and the variants are described below (Fig. 7).

The association between Mg*DDX21 gene polymorphisms and bacterial resistance of oyster*

The association between sequence polymorphisms and bacterial resistance was investigated by examining the distribution and frequency of 25 promoter SNP sites in bacterial resistant and common populations. Sequencing profile analysis revealed that homozygous genotypes had single peaks, while heterozygous genotypes had overlapping peaks (Fig. S1). For instance, the sequencing profiles of two genotypes -3685 GG and -3685 CC showed their specific G or C single peaks, respectively, while the sequencing profile of genotype -3243 AC showed overlapping peaks of A and G. Among the 25 polymorphic loci,

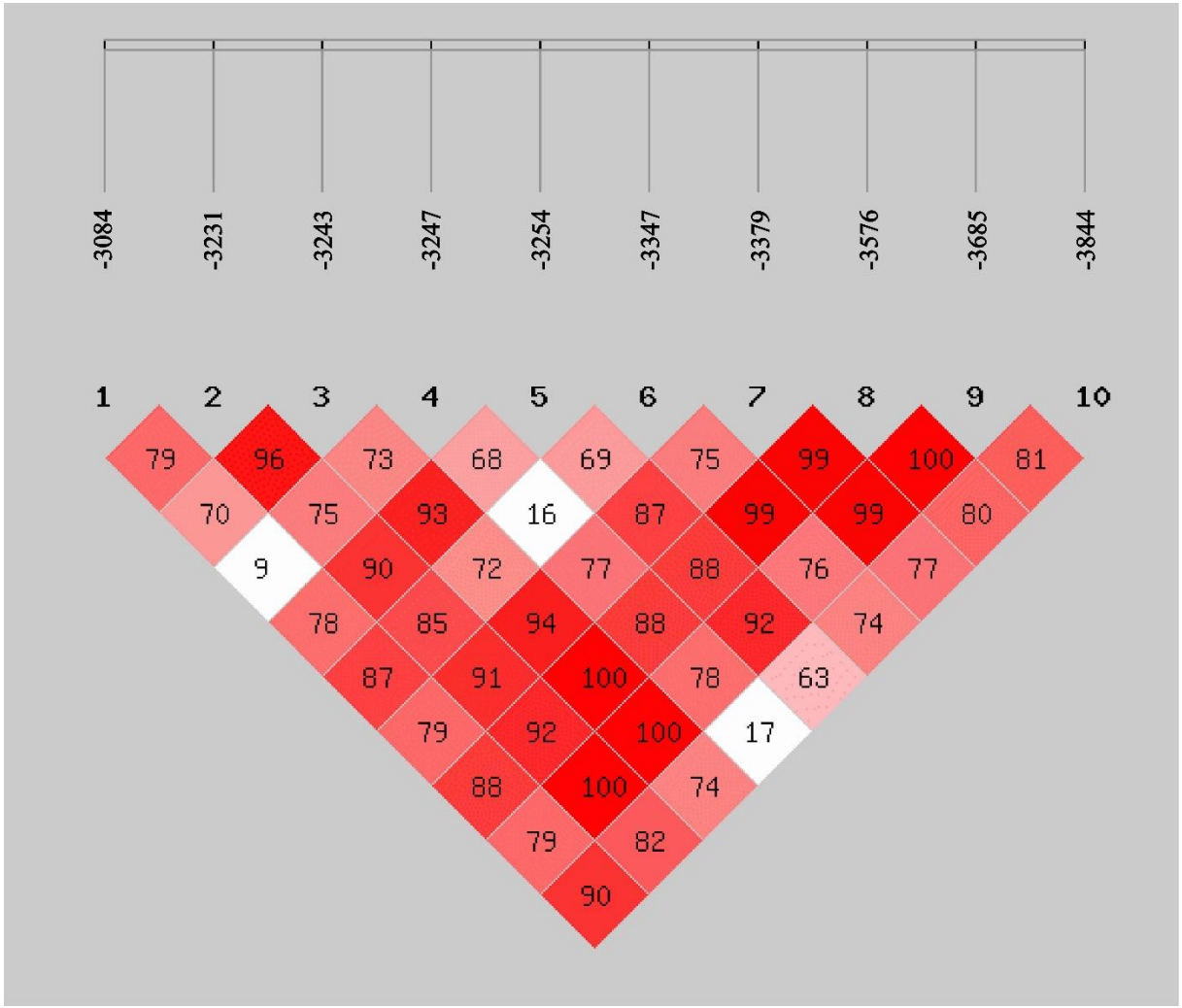

Fig. 8 The linkage disequilibrium analysis of the ten SNPs in the promoter region of *Mg*DDX21. SHEsis software (http://analysis2.bio-x.cn/myAnalysis.php) was used forthis analysis. The color scheme is white (D = 0), pink (0 < D < 1), and red (D = 1) (color figure online)

each locus formed three genotypes reflected by three kinds of sequencing maps (Fig. S1，Table 3).

The HWE for genotype frequencies was analyzed with the goodness-of-fit χ^2-test. Statistical analysis revealed that the genotype frequency of alleles at 11 loci (-3628, -3135, -2985, -2992, -3001, -3079, -3093, -3562, -3053, -2996, -3045) were in HWE ($P > 0.05$) in the common population, while not in HWE ($P < 0.05$) in the bacterial-resistant population. Additionally, 14 loci (-3685, -3576, -3231, -3844, -3515, -3254, -3084, -3247, -3347, -3379, -3243, -3597, -3593, -2994) were not in HWE ($P < 0.05$) in both populations (Table 2).

The allele and genotype frequencies of 25 loci within the *Mg*DDX21 promoter region were summarized in Table 3. Allele and genotype frequencies at loci -3593 and -2994 showed no significant statistical difference between the two populations ($P > 0.05$). The allele frequency at locus -3597 did not significantly differ between common populations ($P > 0.05$), whereas genotype frequencies did ($P < 0.05$) between bacterial-resistant populations. The allele and genotype frequencies at 21 loci (-3844, -3685, -3628, -3576, -3562, -3515, -3379, -3347, -3254, -3247, -3243, -3231, -3135, -3093, -3084, -3079, -3053, -3045, -3001, -2992 and -2985) were all significantly different between two populations ($P < 0.05$). The frequencies of individuals with genotypes -3844 T/T, -3685 C/C, -3628 TT, -3576 A/A, -3562 A/A, -3515 A/A, -3379 A/A, -3347 T/T, -3254 C/C, -3247 A/A, -3243 C/C, -3231 A/A, -3135 T/T, -3093 C/C, -3084 T/T, -3079 T/T, -3053 T/T, -3045 A/A, -3001 A/A, -2992 T/T and -2985 C/C in the bacterial-resistant population were significantly higher than those in the common population ($P < 0.05$) (Table 2).

The result of the pair-loci LD (linkage disequilibrium) test revealed that the loci in *Mg*DDX21 gene promoter were in different degrees of LD. From the 25 SNP loci mentioned, the 10 loci (-3084, -3231, -3243, -3247, -3254, -3347, -3379, -3576, -3685, -3844) were selected for LD analysis. It worths noting that except for the pairs involving loci -3084 and -3247, -3347 and -3247, and -3844 and

Table 4 The haplotype analysis of *Mg*DDX21 polymorphic loci -3084, -3231, -3243, -3247, -3254, -3347, -3379, -3576, -3685 and -3844 in the common and bacterial-resistant populations

Number	Haplotype	Common population (frequency)	Bacterial-resistant population (frequency)	χ^2 (*P*)
1	T A C A C T A A C T	0.000	0.500↑	34.297（*P* < 0.05）
2	G G A A T G C T G C	0.276	0.000↓	14.283（*P* < 0.05）
3	G G A C T G C T G C	0.172	0.000↓	8.289（*P* < 0.05）
4	T G A A T G C T G T	0.103	0.000↓	4.747（*P* < 0.05）

-3247, the remaining pairs exhibit a certain degree of LD with a pairwise D' > 0.60 (Fig. 8). Considering that the LD between different polymorphic loci in one gene usually form different haplotypes, haplotype analysis was conducted on the aforementioned 10 loci. They formed 4 haplotypes with frequency greater than 0.01, and the frequency of haplotype TACACTAACT in bacterial-resistant population was significantly higher than that in common population ($P < 0.05$), while the frequency of haplotype GGAATGCTGC in common population was significantly higher than that in bacterial-resistant population ($P < 0.05$) (Table 4).

Discussion

Although RNA helicase is not the only factor influencing bacterial resistant traits, organisms may employ various strategies to resist pathogens. The expression of RNA helicase still shows a strong correlation with disease resistance traits (Tapescu and Cherry, 2024). In mammalian studies, DDX21 has been shown to maintain innate immune homeostasis by negatively regulating IFN-β production (Li *et al*., 2022). Additionally, it contributes to genomic stability by promoting DNA damage repair, thereby participating in cellular immune regulation (Wang *et al.,* 2024). In this study, the protein structure, evolutionary relationship, as well as the mRNA expression profile of *Mg*DDX21 were characterized. The predicted *Mg*DDX21 protein contains a classical DEXDc domain, a HELICc domain and a GUCT domain, as well as the key motifs and functional sites, which are similar to the DDX21 from human (Flores-Rozas and Hurwitz, 1993). Interestingly, the repetitive sequence at the C-terminus was not identified in *Mg*DDX21, which is unique to mammals such as humans and rodents, suggesting species-specific adaptations (Xiao *et al*., 2024). Moreover, the amino acid sequences especially the conserved ATP binding, RNA binding, and domain-domain interactions sites are highly conserved among different species (Chen *et al*., 2020).

In order to investigate the function of *Mg*DDX21 in immune response of oysters, their expression levels in haemocytes and different tissues, as well as after high-temperature and LPS treatment were detected. *Mg*DDX21 was widely distributed in haemocytes and all the examined tissues. It is well known that oysters possess an opening circulatory system, and circulating haemocytes is of vital importance in participating in immune response and effectively eliminating invading pathogens (Cochennec-Laureau *et al*., 2003; Lannig, Flores and Sokolova, 2006; Wang *et al*., 2018). Moreover, several studies have showed the involvement of DDX21 in regulating innate immunity of cells and maintaining innate immune homeostasis by negatively regulating the production of IFN-b (Abdullah *et al*., 2021; Li *et al*., 2022). Therefore, the high expression level and the significantly upregulation by high-temperature and LPS treatment in haemocytes implied that *Mg*DDX21 might play important roles in immune response of oyster.

Considering that the transcriptional regulation of gene expression depends on the interaction between transcription factors and the putative cis-acting elements in the promoter region of genes, a fragment of 2272 bp in the remote promoter region of *Mg*DDX21 was amplified from oyster to analyze the reason for its induction expression by LPS, and some putative binding sites were identified, such as HSF, FOXO and SPI1. These transcription factors, which are highly relevant to immune responses, may be involved in immune regulation after stimulation by pathogenic bacteria through the modulation of expression of a variety of genes or signal paths. For instance, HSF-1 indirectly sustains immune-cell function by maintaining protein homeostasis through its regulation on heat-shock response (Kovács *et al*., 2024). Both SPI1 and FOXO can regulate the fate of immune cells and the balance of inflammation through transcriptional networks, and their activation or inhibition can both become new targets for precisely regulating inflammatory diseases (Peng, 2008; Zhu *et al*., 2023). All these results indicated that *Mg*DDX21 plays important roles in responding to bacterial stimulation. Variations in the promoter sequence can affect its affinity for transcription factor, thereby influencing the levels of gene expression. The differences in disease resistance of individual animals may be partly attributed to the existence of polymorphisms in a series of related genes (Zhang *et al*., 2021). This study identified 12 SNP sites in the promoter region of the DDX21 gene that alter certain transcription factor binding sites, potentially affecting transcription efficiency. This hypothesis may partially explain the differential expression patterns of DDX21 mRNA in two oyster species after high-temperature treatment and LPS stimulation.

Considering that SNPs in the promoter region of the *Mg*DDX21 gene could explain the variation in bacterial resistance between the two populations, association analysis was conducted to examine the relationship between these SNPs and the oysters' bacterial resistance through a case-control study approach (Hoh *et al*., 2001). Statistics indicate that the genotype frequencies at the 25 SNP sites in the bacterial resistant populations are significantly different in the HWE population ($P < 0.05$). Mutational events are typically followed by environmental selection (Tanguy and Moraga, 2001), which may be evident through deviations from HWE (Schaid and Jacobsen, 1999), the disequilibrium of the genotype frequency at the 25 loci in the *Mg*DDX21 promoter region might imply a genetic adaptation process. In order to verify this extrapolation, the allele and genotype frequencies at fourteen loci in the *Mg*DDX21 promoter region were calculated and compared. Among these 25 sites, 21 SNPs (-3844T/T, -3685C/C, -3628TT, -3576A/A, -3562A/A, -3515A/A, -3379A/A, -3347T/T, -3254C/C, -3247A/A, -3243C/C, -3231A/A, -3135T/T, -3093C/C, -3084T/T, -3079T/T, -3053T/T, -3045A/A, -3001A/A, 2992T/T and -2985C/C) exhibit significant differences in allele and genotype frequencies between the two populations ($P < 0.05$), and they could be considered as the candidate loci related to disease resistance. The characterization of such mutation has important implications for understanding of the genetic adaptation processes in organisms (Kovács *et al*., 2024).

As most of the resistance traits are of quantitative and they are always controlled by multiple genes (Zeng, 1993), the contribution of a single SNP might be a small part of the related traits. This study explores the potential interaction between genotype and bacterial resistance through LD and haplotype analysis of SNPs in the promoter region of the *Mg*DDX21. By examining the associations between specific SNPs and resistance traits, we aim to identify genetic factors that may contribute to enhanced disease resistance. From the 25 SNPs, we selected the 10 sites (-3084, -3231, -3243, -3247, -3254, -3347, -3379, -3576, -3685, -3844) for LD analysis. The results indicate varying degrees of LD among these sites in the DDX21 gene promoter, with the exceptions of sites -3084 and -3247, -3347 and -3247, and -3844 and -3247, which exhibit lower linkage. All other pairs show strong LD. The LD between different polymorphic loci in one gene usually leads to the formation of different haplotypes, so a haplotype analysis was conducted on the aforementioned 10 sites. The results showed that these 10 polymorphic sites can form 4 haplotypes. Notably, the TACACTAACT haplotype was significantly more prevalent in the bacterial resistant populations compared to the common populations, indicating that the TACACTAACT haplotype confers stronger disease resistance to oysters compared to other haplotypes.

In summary, the mRNA expression of *Mg*DDX21 gene in oysters was responsive to LPS stimulation, significant association between the promoter polymorphisms and bacterial resistance was established in bacterial-resistant population, and some potential gene markers associated with enhanced bacterial resistance could be applied in the future molecular assisted selection program of oysters. The present results indicated that the peculiarities of DDX21 gene expression was closely related to oyster resistance to pathogenic bacteria. However, results presented in this study are relatively preliminary, and further researches are still needed to conduct direct functional validation of the identified SNPs.

Acknowledgements

We are grateful to all the laboratory members for their technical advice and helpful discussions. This research was supported by National Natural Science Foundation of China (32230110), the fund for CARS-49 in MARA, the National Key R&D Program (2018YFD0900601), and Dalian High Level Talent Innovation Support Program (2022RG14).

References

Abdullah SW, Wu J, Zhang Y, Bai M, Guan J, Liu X, *et al*. DDX21, a Host Restriction Factor of FMDV IRES-Dependent Translation and Replication. Viruses. 13(9), 2021.

Bamezai R. Bloom syndrome: is the gene mapped to the point? Indian J Exp Biol. 34(4): 298-301, 1996.

Calo E, Flynn RA, Martin L, Spitale RC, Chang HY, Wysocka J. RNA helicase DDX21 coordinates transcription and ribosomal RNA processing. Nature. 518(7538): 249-253, 2015.

Chen Z, Li Z, Hu X, Xie F, Kuang S, Zhan B, *et al*. Structural Basis of Human Helicase DDX21 in RNA Binding, unwinding, and antiviral signal activation. Adv Sci (Weinh). 7(14): 2000532, 2020.

Cochennec-Laureau N, Auffret M, Renault T, Langlade A. Changes in circulating and tissue-infiltrating hemocyte parameters of European flat oysters, *Ostrea edulis*, naturally infected with *Bonamia ostreae*. J Invertebr Pathol. 83(1): 23-30, 2003.

Cordin O, Banroques J, Tanner NK, Linder P. The DEAD-box protein family of RNA helicases. Gene. 367: 17-37, 2006.

Fairman-Williams ME, Guenther UP, Jankowsky E. SF1 and SF2 helicases: Family matters. Curr Opin Struct Biol. 20(3): 313-324, 2010.

Flores-Rozas H, Hurwitz J. Characterization of a new RNA helicase from nuclear extracts of HeLa cells which translocates in the 5' to 3' direction. J Biol Chem. 268(28): 21372-21383, 1993.

Gan Z, Cheng J, Hou J, Xia H, Chen W, Xia L, *et al*. Molecular and functional characterization of tilapia DDX41 in IFN regulation. Fish Shellfish Immunol. 99: 386-391, 2020.

Guo J, Hong F, Loke J, Yea S, Lim CL, Lee U, *et al*. A DDX5 S480A polymorphism is associated with increased transcription of fibrogenic genes in hepatic stellate cells. J Biol Chem. 285(8): 5428-5437, 2010.

Hoh J, Wille A, Ott J. Trimming, weighting, and grouping SNPs in human case-control association studies. 11(12): 2115-2119, 2001.

Hu A, Wang Y, Tian J, Chen Z, Chen R, Han X, *et al*. Pan-cancer analysis reveals DDX21 as a

potential biomarker for the prognosis of multiple tumor types. Front Oncol. 12: 947054, 2022.
Kovács D, Biró JB, Ahmed S, Kovács M, Sigmond T, Hotzi B, *et al*. Age-dependent heat shock hormesis to HSF-1 deficiency suggests a compensatory mechanism mediated by the unfolded protein response and innate immunity in young *Caenorhabditis elegans*. Aging Cell. 23(10): e14246, 2024.
Lannig G, Flores JF, Sokolova IM. Temperature-dependent stress response in oysters, *Crassostrea virginica*: Pollution reduces temperature tolerance in oysters. Aquat Toxicol. 79(3): 278-287, 2006.
Li C. Isolation and identification of a pathogenic strain of *Halomonas* from the aquaculture environment breeding the *Crassostrea gigas* larvae. Dalian: Dalian Ocean University (in Chinese), 2022.
Li J, Fang P, Zhou Y, Wang D, Fang L, Xiao S. DEAD-box RNA helicase 21 negatively regulates cytosolic RNA-mediated innate immune signaling. Front Immunol. 13: 956794, 2022.
Ma X, Lu T, Yang Y, Qin D, Tang Z, Cui Y, *et al*. DEAD-box helicase family proteins: emerging targets in digestive system cancers and advances in targeted drug development. J Transl Med. 22(1): 1120, 2024.
Peng SL. Foxo in the immune system. Oncogene. 27(16): 2337-2344, 2008.
Sarkar M, Ghosh MK. DEAD box RNA helicases: crucial regulators of gene expression and oncogenesis. Front Biosci (Landmark Ed). 21(2): 225-250, 2016.
Schaid DJ, Jacobsen SJ. Biased tests of association: comparisons of allele frequencies when departing from Hardy-Weinberg proportions. Am J Epidemiol. 149(8): 706-711, 1999.
Shih JW, Lee YH. Human DExD/H RNA helicases: emerging roles in stress survival regulation. Clin Chim Acta. 436: 45-58, 2014.
Tanguy A, Moraga D. Cloning and characterization of a gene coding for a novel metallothionein in the Pacific oyster *Crassostrea gigas* (*Cg*MT2): a case of adaptive response to metal-induced stress? Gene. 273(1): 123-130, 2001.
Tapescu I, Cherry S. DDX RNA helicases: key players in cellular homeostasis and innate antiviral immunity. J Virol. 98(10): e0004024, 2024.
Tseng TL, Wang YT, Tsao CY, Ke YT, Lee YC, Hsu HJ, *et al*. The RNA helicase DDX52 functions as a growth switch in juvenile zebrafish. Development. 148(15), 2021.
Valdez BC, Yang H, Hong E, Sequitin AM. Genomic structure of newly identified paralogue of RNA helicase II/Gu: detection of pseudogenes and multiple alternatively spliced mRNAs. Gene. 284(1-2): 53-61, 2002.
Wang L, Song X, Song L. The oyster immunity. Dev Comp Immunol. 80: 99-118, 2018.
Wang Q, Cao R, Ning X, You L, Mu C, Wang C, *et al*. Effects of ocean acidification on immune responses of the Pacific oyster *Crassostrea gigas*. Fish Shellfish Immunol. 49: 24-33, 2016.
Wang S, Yang R, Song M, Li J, Zhou Y, Dai C, *et al*. Current understanding of the role of DDX21 in orchestrating gene expression in health and diseases. Life Sciences. 349: 122716, 2024.
Wu W, Sun J, Dong M, Yang Q, Yang W, Zhang T, *et al*. *Cg*TNF-2 promotes the proliferation of haemocytes by regulating the expressions of *Cg*Runx and cell cycle related genes in the Pacific oyster *Crassostrea gigas*. Fish Shellfish Immunol. 132: 108478, 2023.
Xiao Y, Fan J, Li Z, Hou Y. DDX21 at the Nexus of RNA Metabolism, Cancer Oncogenesis, and Host-Virus Crosstalk: Decoding Its Biomarker Potential and Therapeutic Implications. Int J Mol Sci. 25(24), 2024.
Yajima M, Wessel GM. The DEAD-box RNA helicase Vasa functions in embryonic mitotic progression in the sea urchin. Development. 138(11): 2217-2222, 2011.
Yang C, Wang L, Wang J, Jiang Q, Qiu L, Zhang H, *et al*. The polymorphism in the promoter of HSP70 gene is associated with heat tolerance of two congener endemic bay scallops (*Argopecten irradians irradians* and *A. i. concentricus*). PLoS One. 9(7): e102332, 2014.
Zeng ZB. Theoretical basis for separation of multiple linked gene effects in mapping quantitative trait loci. Proc Natl Acad Sci U S A. 90(23): 10972-10976, 1993.
Zhang Y, Liu J, Wang C, Liu J, Lu W. Toll-Like Receptors Gene Polymorphisms in Autoimmune Disease. Front Immunol. 12: 672346, 2021.
Zhou J, Zhao J, Sun H, Dai B, Zhu N, Dai Q, *et al*. DEAD-box RNA helicase 21 interacts with porcine circovirus type 2 Cap protein and facilitates viral replication. Front Microbiol. 15: 1298106, 2024.
Zhu J, Gao X, Li Y, Zhang Z, Xie S, Ren S, *et al*. Human FAM111A inhibits vaccinia virus replication by degrading viral protein I3 and is antagonized by poxvirus host range factor SPI-1. Proc Natl Acad Sci U S A. 120(35): e2304242120, 2023.

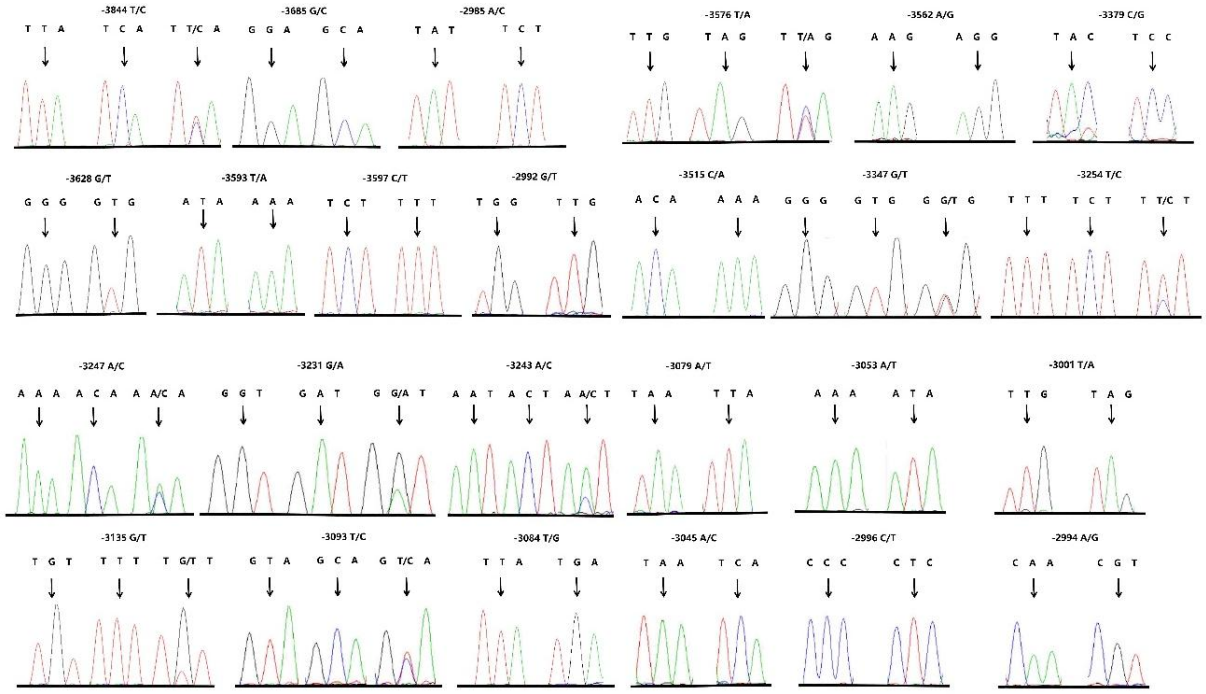

Fig. S1 Detection of the genotypes at twenty-five SNPs in the *Mg*DDX21 promoter region. The unimodal peak indicates the homozygous genotype, and the overlapping peaks indicate the heterozygous genotype